The Effect of Quartz Particle Size and Melt Viscosity on HLW Melter Feed Using Pellet Test Response – 16226

SeungMin Lee [a], Zachary Hilliard [a], Jayven S. Heilman-Moor [a], Charles C. Bonham [a], Derek R. Dixon [a], Pavel Hrma [a], Michael J. Schweiger [a], and Albert A. Kruger [b]

[a] Pacific Northwest National Laboratory Richland, Richland, WA 99352

[b] U.S. Department of Energy, Office of River Protection, Richland, WA 99352

ABSTRACT

Melter performance is affected by various physical and chemical parameters of the feed. To study the effect of these parameters on waste glass melting efficiency, we monitored the volume expansion of feed pellets in response to heating. This study focuses on the effects of quartz particle size and melt viscosity on a simplified high-alumina high-level waste melter feed labeled A19. In this research the A19 feed was prepared with eight different partitions of quartz particle size ranging from 5 to 250 µm and six modified A19 feeds were formulated to produce melts of viscosities that varied from 1 to 30 Pa s at 1050°C. The volume change of the pellets was monitored with a camera and the volume of pellets was calculated from the profile area of the images. Collected data were then analyzed to characterize the melting behavior of the feed. The low-temperature expansion of the pellet from 400°C to 600°C, a temperature interval at which complex feed reactions occur, was reduced with increasing quartz particle size and viscosity. Foaming occurred from 800°C to 1000°C as the pores were sealed by the connected glass-forming melt. Small sizes of quartz particles caused excessive foaming and earlier onset of foaming, in comparison to larger quartz particle sizes. As is well known, too small or too big quartz particles and high melt viscosity inhibit the rate of melting.

INTRODUCTION

The Hanford Site, in Washington State, has 177 underground waste storage tanks that contain over 0.2 million m^3 of radioactive waste. The Hanford Tank Waste Treatment and Immobilization Plant, currently under construction, will immobilize both high-level waste (HLW) and low-activity waste (LAW) in borosilicate glass. These wastes will be mixed with glass-forming additives to make feed that will be charged into electric melters. The feed is charged on top of a pool of molten glass, where it forms a reacting semi-solid layer called a cold cap [1] where various chemical reactions and physical transformations occur [2, 3] and affect the rate of melting [2, 4, 5] via physical and chemical parameters such as the mineralogical form of glass additives, the particle size of solids, the loading and type of waste, and the melter feed rheology [2]. These parameters influence the waste glass melting efficiency by the determining the heat transfer within the cold cap. The

volume expansion of feed in response to heating is indicative of foaming behavior. Foam occurs between the main body of the cold cap and the melt pool, thus producing an undesirable thermally insulating effect that has an adverse impact on the rate of melting. In this work, the volume expansion of melter feeds was monitored by observing the volume change of feed pellets that occur in response to increasing temperature. This study focuses on the effects of quartz particle size and melt viscosity on melting behavior, via the pellet test, of a simplified high-alumina HLW melter feed labelled A19. In one series of experiments, the feed was prepared with eight different ranges of quartz particle size ranging between 5 and 250 µm. In addition, modified A19 feeds were formulated to produce melts of viscosities that varied from 1 to 30 Pa s at 1050°C.

EXPERIMENTAL PROCEDURE

Preparation of Batches

Table 1 shows the compositions of the batches used in this research. The glass compositions are listed in Table 2. Batches of the A19-original feed were used to study the effects of quartz particle size. The A19 modified feeds (A19-0 to A19-9) were formulated to achieve different melt viscosities. All feeds would produce a simplified high-alumina HLW glass. To prepare slurries 800 ml deionized H_2O was used for A19-original batch (in the amount equivalent to 400 g glass, see Table 1) and 400 ml for the remaining batches (each equivalent to 250 g glass). Batch slurries were prepared from all chemicals except quartz and dried in the oven at 105°C overnight. The dried batches were milled to powder. The effects of quartz particle size were also determined for feed containing 22 wt% SiO_2 with all other components at the same proportions as in the A19-original feed (containing 27 wt% SiO_2, see Table 1).

TABLE 1. Compositions of A19 Batches in g to make 400 g A19-original glass and 250 g modified glasses

Compound	A19-original	A19-0	A19-1	A19-5	A19-7	A19-9
$Al(OH)_3$	148.71	92.95	92.95	92.95	92.95	92.95
$B(OH)_3$	136.63	107.94	95.22	80.19	76.60	73.87
Bi_2O_3	4.67	2.92	2.92	2.92	2.92	2.92
CaO	4.35	2.72	2.72	2.72	2.72	2.72
$Cr_2O_3 \cdot 1.5H_2O$	2.48	1.55	1.55	1.55	1.55	1.55
NaF	6.00	3.75	3.75	3.75	3.75	3.75
$Fe(OH)_3$	29.75	18.60	18.60	18.60	18.60	18.60
Li_2CO_3	35.69	28.19	24.87	20.95	20.01	19.29
$Ni(OH)_2$	2.01	1.26	1.26	1.26	1.26	1.26
$Fe(H_2PO_2)_3$	5.01	3.13	3.13	3.13	3.13	3.13

PbO	1.67	1.04	1.04	1.04	1.04	1.04
SiO_2	88.58	37.86	47.74	59.41	62.19	64.31
Na_2SO_4	1.44	0.90	0.90	0.90	0.90	0.90
$Zr(OH)_4$	2.21	1.38	1.38	1.38	1.38	1.38
$CaSiO_3$	38.83	24.27	24.27	24.27	24.27	24.27
NaOH	7.95	4.97	4.97	4.97	4.97	4.97
Na_2CO_3	42.63	33.68	29.71	25.02	23.90	23.05
$NaNO_2$	1.39	0.87	0.87	0.87	0.87	0.87
$NaNO_3$	4.96	3.10	3.10	3.10	3.10	3.10
$Na_2C_2O_4$	0.50	0.32	0.32	0.32	0.32	0.32
Total	565.47	371.38	361.24	349.26	346.41	344.23

TABLE 2. Compositions of Glass (in Mass Fractions) and Their Model-Estimated Viscosity

Compound	**A19-original**	**A19-0**	**A19-1**	**A19-5**	**A19-7**	**A19-9**	**A19-11**
Al_2O_3	0.2420	0.2420	0.2420	0.2420	0.2420	0.2420	0.2420
B_2O_3	0.1919	0.2426	0.2140	0.1802	0.1722	0.1660	0.1610
Bi_2O_3	0.0116	0.0116	0.0116	0.0116	0.0116	0.0116	0.0116
CaO	0.0559	0.0559	0.0559	0.0559	0.0559	0.0559	0.0559
Cr_2O_3	0.0053	0.0053	0.0053	0.0053	0.0053	0.0053	0.0053
F	0.0067	0.0067	0.0067	0.0067	0.0067	0.0067	0.0067
Fe_2O_3	0.0596	0.0596	0.0596	0.0596	0.0596	0.0596	0.0596
Li_2O	0.0357	0.0452	0.0398	0.0335	0.0320	0.0309	0.0300
Na_2O	0.0961	0.1215	0.1072	0.0903	0.0862	0.0832	0.0807
NiO	0.0040	0.0040	0.0040	0.0040	0.0040	0.0040	0.0040
P_2O_5	0.0106	0.0106	0.0106	0.0106	0.0106	0.0106	0.0106
PbO	0.0041	0.0041	0.0041	0.0041	0.0041	0.0041	0.0041
SiO_2	0.2704	0.1849	0.2332	0.2902	0.3038	0.3141	0.3225
SO_3	0.0020	0.0020	0.0020	0.0020	0.0020	0.0020	0.0020
ZrO_2	0.0040	0.0040	0.0040	0.0040	0.0040	0.0040	0.0040
Total	1.00	1.00	1.00	1.00	1.00	1.00	1.00
η(Pa s)@1050°C	8.94	1.09	3.58	14.53	20.30	26.20	32.20
η(Pa s)@1150°C	3.49	0.49	1.49	5.49	7.49	9.49	11.49

Preparation of Quartz Particles of Different Size Fractions

Quartz particles of size fractions listed in Table 3 were prepared from SIL-CO-SIL 250 by sieving and SIL-CO-SIL 5 was used for silica particle size less than or equal to 5 µm. The fractions were washed in deionized water followed by washes with ethanol using an ultrasonic cleaner and dried in the oven at 90°C for an hour. Quartz particle size fraction of 63 to 75 µm was used for the viscosity series.

TABLE 3. Quartz Particle Size Fractions

Source	Range (µm)
SIL-CO-SIL 250	106 - 250
	90 - 106
	75 - 90
	63 - 75
	45 - 63
	25 - 45
	1 - 25
SIL-CO-SIL 5	1 - 5

Preparation of Pellet Samples

Samples of A19-original dry feed (and the 22 wt% SiO_2 alternative) were manually mixed with eight different quartz particle sizes (Table 3) and pressed into pellets at 168 MPa for 90 seconds. Pellets were circular disks 1.5 g in weight, 13 mm in diameter, and 6 mm thick. Pellets for modified feeds were prepared in the same manner.

Pellet Test for Volume Expansion

A pellet was loaded in the high-temperature furnace on an alumina plate of 33 mm in diameter and 2.5 mm thick. The furnace was heated to 1100°C at 10 K min^{-1} while the profile of the pellet was monitored with a camera through a quartz-glass window in the side wall of the furnace. Fig. 1 shows the shape change of pellets for A19-original and A19-9 feeds.

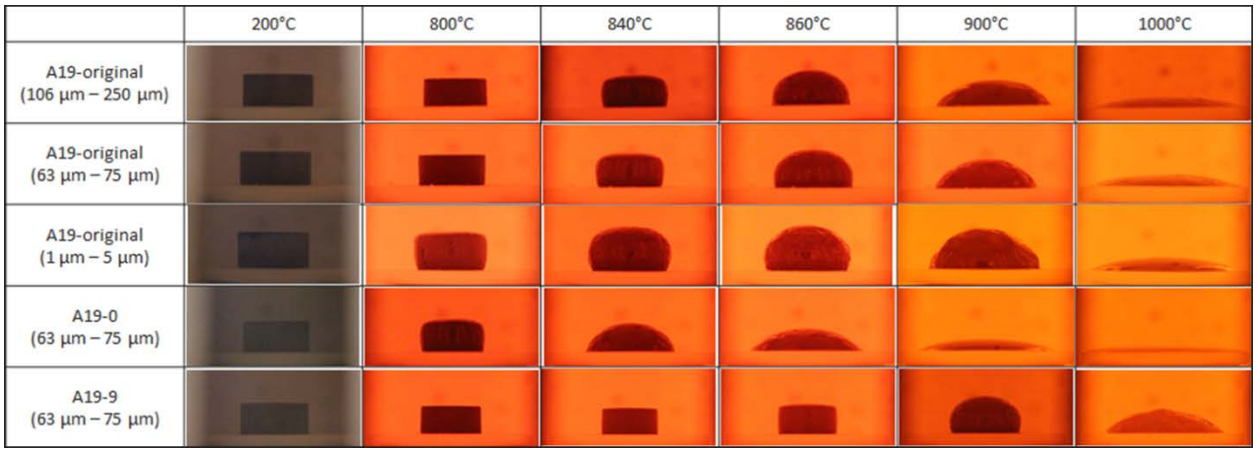

Fig. 1. Profiles of Pellets Made from A19-original and A19-9 Dried Feeds.

Viscosity Test with Glass Batches

The A19 series were designed using a viscosity model [6, 7]. Starting from the A19-original glass, SiO_2 was changed for B_2O_3 + Na_2O + Li_2O kept in the same proportions in all compositions. As seen in Table 2, glasses were formulated for

viscosity to vary by 2 Pa s (except A19-0) at 1150°C. The glasses were then prepared from dry chemicals, melted in a covered platinum crucible for 1 hour at 1150°C, milled to powder, remelted. The viscosity was measurement using a rotating spindle viscometer.

RESULT AND DISCUSSION

Analysis of Volume Expansion

Fig. 2 shows pellets heated to 1100°C. As Fig. 2 (a) shows, the feed with small silica particles left small bubble traces on the melt surface, whereas the feed with large silica particles produced larger bubbles causing a rough surface. This is because small size of silica is dissolved in the melting feed faster and bubble trapped in the melting feed longer affects the melt mobility. As Fig. 2 (b) shows, the high-viscosity melt had rough surface with large bubble traces, whereas the low-viscosity melt had a smooth surface, which is as expected [9, 11].

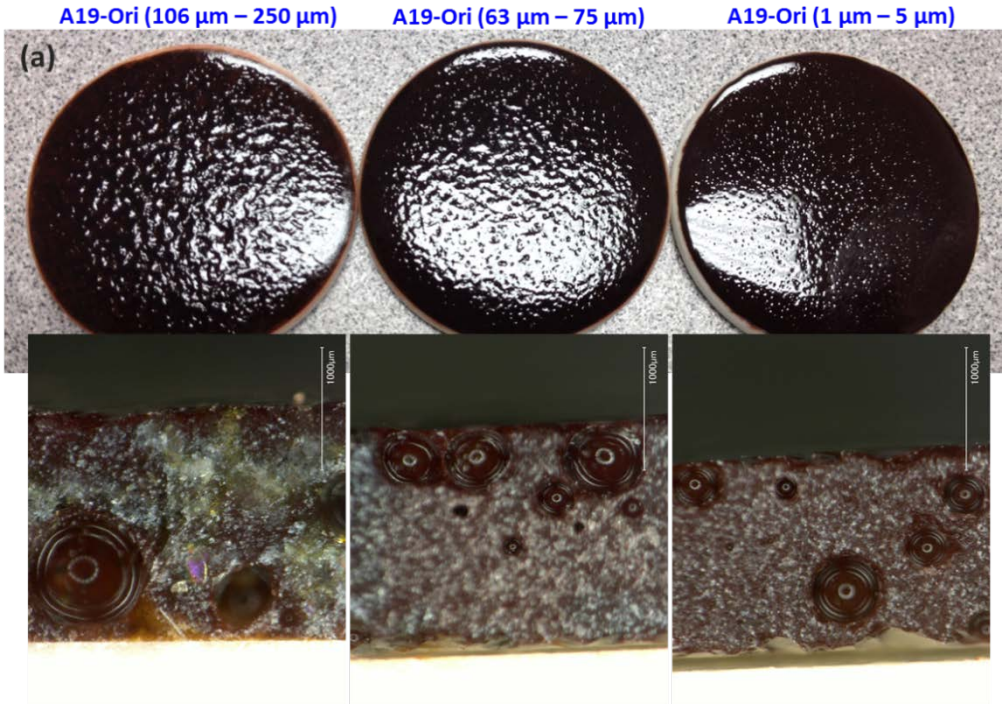

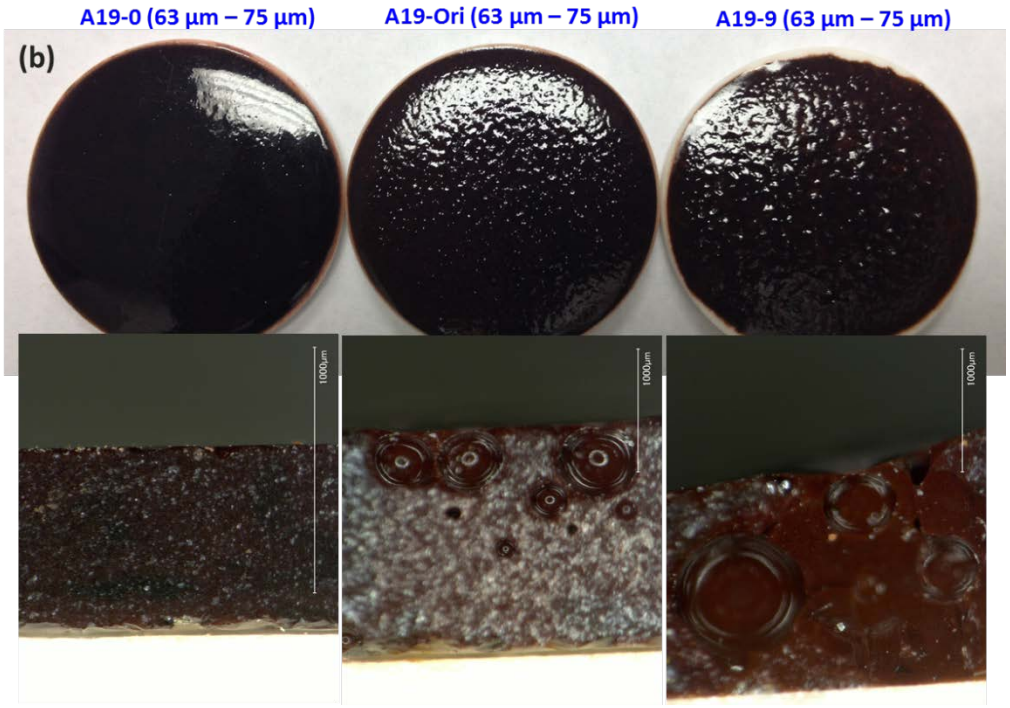

Fig. 2. Pictures of Pellets after Heating to 1100°C: (a) A19-original Feed with Three Different Silica Particle Sizes and (b) Three Different A19 Series Feeds with 63-75 µm Silica Size Fraction.

The volume of the pellet was obtained by numerical integration using the pellet profile (Fig. 1) in the pictures taken by the camera [8, 9]. Each picture of a pellet was processed with Photoshop®[a] software and the MATLAB®[b] program [10].

Effect of Quartz Particle Size

Fig. 3 shows the normalized volume of A19-original feed with different quartz particle sizes and Fig. 4 displays the parameters of major maxima and minima as functions of the average silica particle size. As expected, feeds with small particles of silica generated more foaming leading to larger volume expansion. The temperatures at which the volume reached a minimum before foaming began increased as the silica particle size increased. The main maxima occurred around 910°C and the initial maxima were shown around 540°C. As shown in Fig. 4, the trend lines correspond with exponential approximation function (except for the constant function for the temperature of maximum volume expansion).

[a] Photoshop® is a registered trademark of Adobe Systems Incorporated in the United States and/or other countries.
[b] MATLAB® is a registered trademark of The MathWorks, Inc. in the United States and/or other countries.

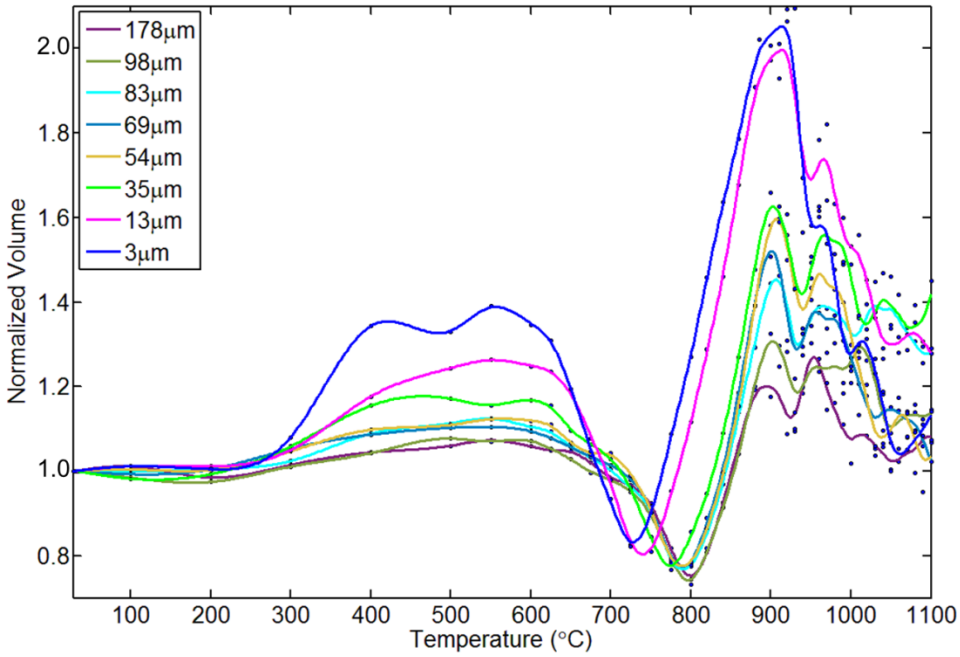

Fig. 3. Normalized Volume of A19-original Feed with Different Quartz Particle Sizes.

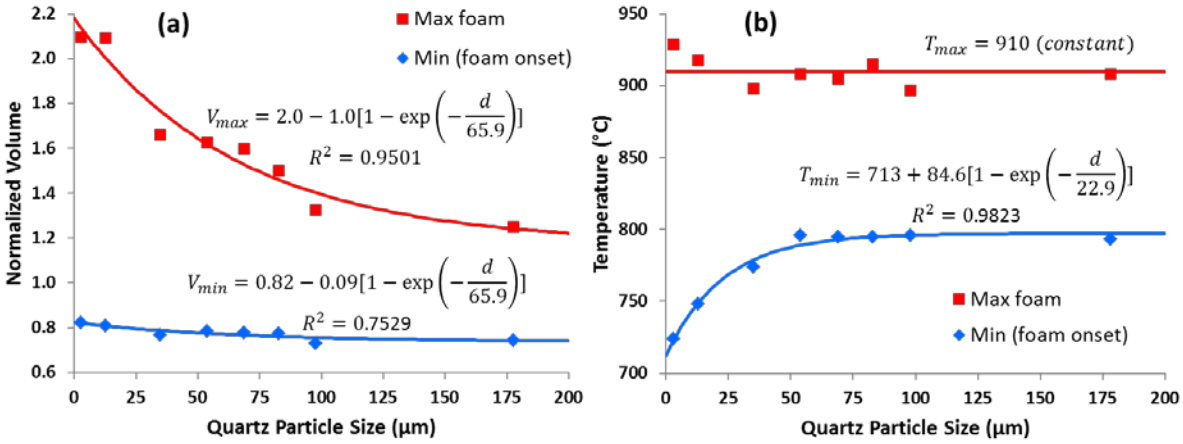

Fig. 4. Maxima and Minima of Normalized Volume and Temperatures (A19-original Feed with Different Quartz Particle Sizes, d): (a) Normalized Volume and (b) Temperature.

Fig. 5 compares experimental data for the 22 wt% SiO_2 fraction in glass with those of 27 wt% SiO_2 fraction (A19-original). A higher silica fraction leads to a higher viscosity and thus a higher volume expansion. Smaller particles dissolve earlier than larger particles. Consequently, higher fractions of small particles of silica increase foaming whereas higher fractions of large particles of silica have an opposite effect.

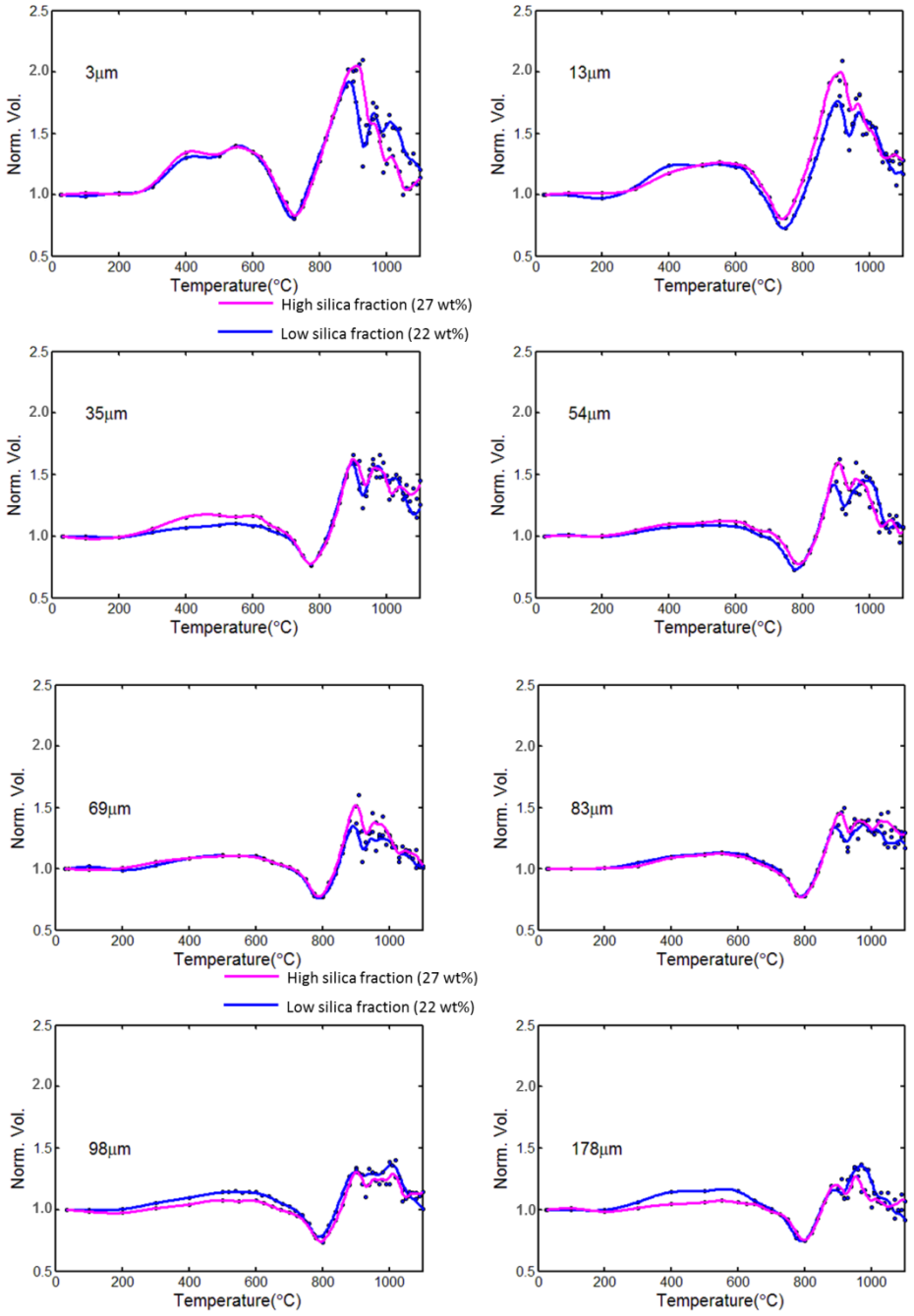

Fig. 5. Comparison of Volume versus Temperature Curves for the 22 wt% SiO_2 Fraction in Glass (blue line) with Those of 27 wt% SiO_2 Fraction (pink line, A19-original) with Various Silica Particle Sizes.

Glass Viscosity

Melt viscosity for A19 glasses was measured at four temperatures, 950, 1050, 1150, and 1250°C. Fig. 6 presents a plot of log viscosity (Pa s) against inverse temperature (K). The relationship is linear.

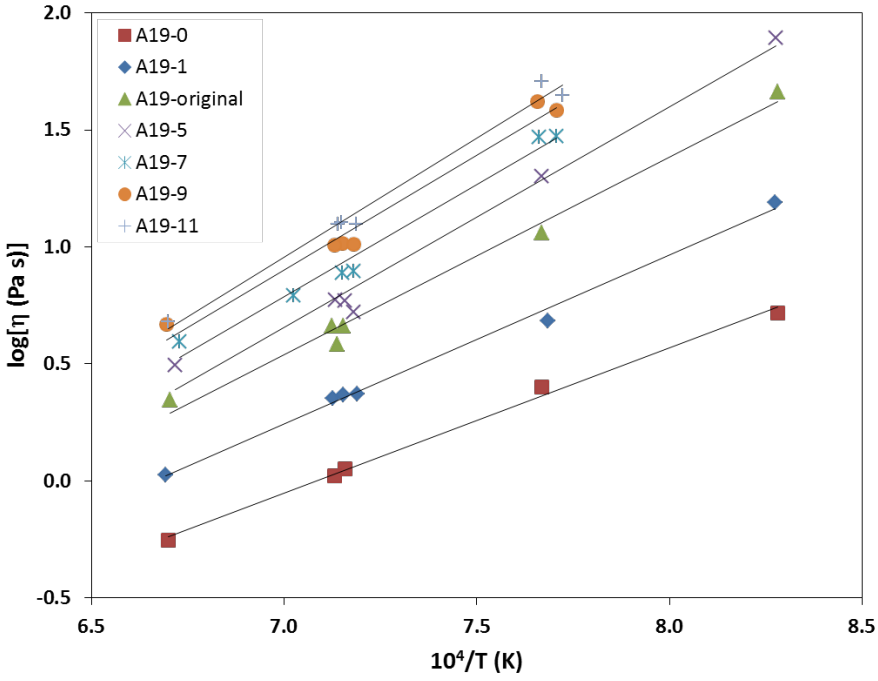

Fig. 6. Measured Viscosity Data with A19-0 through A19-11.

Fig. 7 compares estimated and measured viscosities indicating excellent agreement for high viscosity values at 1050°C. Viscosities < 3.5 Pa s were somewhat underestimated and higher viscosities were slightly overestimated for 1150°C.

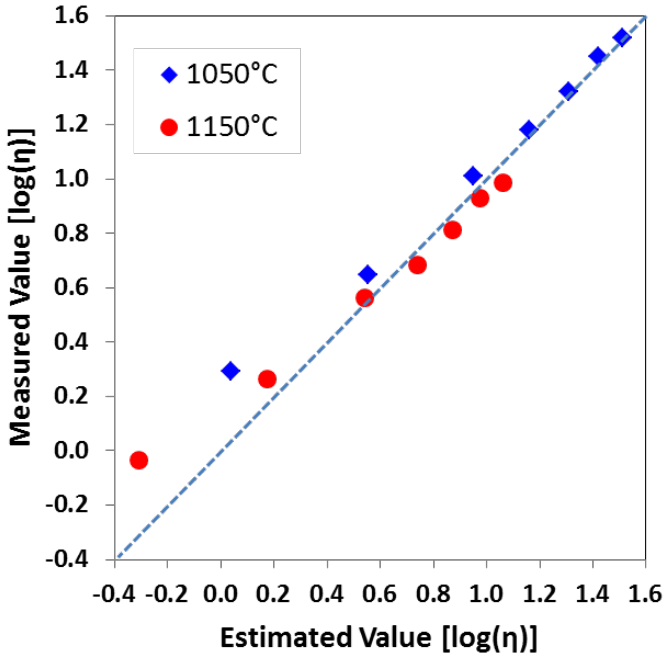

Fig. 7. Comparisons of Viscosity between the Estimated and Measured Data.

Effect of Feed Viscosity

Figs. 8 and 9 display the effect of glass viscosity on the volume expansion of pellets with 63-75 µm quartz particle size. Higher viscosity gives rise to higher volume expansion and earlier onset of foam trapping.

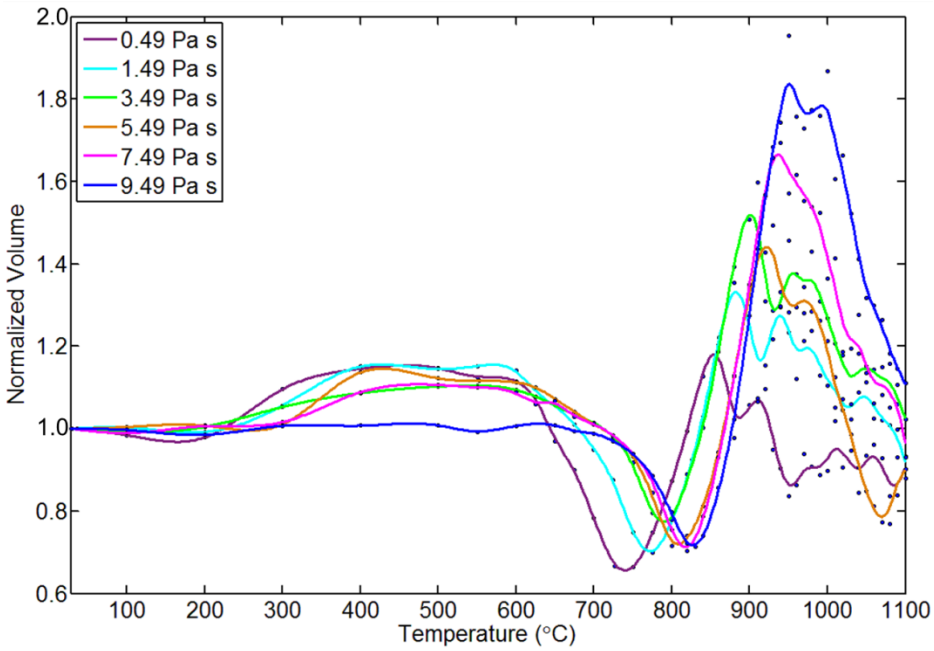

Fig. 8. Normalized Volume of A19 Series Feeds with Different Glass Viscosities (Mixed with Silica of 63 to 75 µm).

Fig. 9 also shows that foaming temperature and maximum volume expansion temperature increases as the viscosity of the glass increases. As shown in Fig. 9, the viscosity curves with normalized volume form a smooth upward slope because the effort was based on viscosity and should have a linear affect. However, the volume expansion temperature does not have this smooth slope (linear) because the variations in chemistry caused the differences in pellet shrinkage and foaming. The trend lines correspond with exponential approximation function (except for the linear function for the maximum volume expansion).

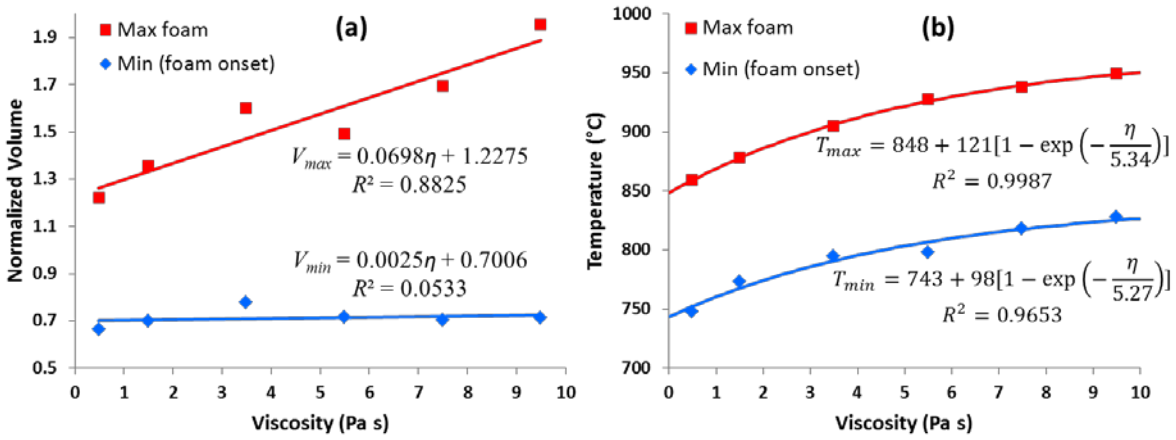

Fig. 9. Maxima and Minima of Normalized Volume and Temperatures (A19 Series Feed with Different Viscosities): (a) Normalized Volume and (b) Temperature.

Relationship between Quartz Particle Size and Viscosity

As shown in Fig. 2 through Fig. 9, feed with fine quartz particles, which dissolve rapidly, generates excessive foam at a lower temperature. On the other hand, feed with large quartz particles, which dissolve slowly, generates less foam but larger bubbles are created that collapse slowly. In addition, feed for high viscosity glass possesses an increased foaming temperature and produces more foam that persists to higher temperature. Feed for low viscosity glass begins to foam at a lower temperature, produces less foam, and collapses earlier. Accordingly, larger quartz particles and lower viscosity are expected to melt faster. Small quartz particles and high viscosity will tend to increase foaming and thus are likely to influence negatively the melting rate. In addition, large sizes of quartz particles are not recommended because they tend to agglomerate a dissolve extremely slowly [11], which can negatively affect melt homogeneity [8, 9].

CONCLUSIONS

In this study, several simulated A19 feeds were batched. Using those feeds, pellet tests with different quartz particle sizes and different viscosities were performed to investigate the volume changes of the specified feed. Massive volume expansion was observed with the finest quartz particle size and high feed viscosity. Fine quartz particle size generated excessive foam because of a rapid dissolution of silica in glass foaming melt. Bubbles created are trapped longer in the high viscosity melt; both conditions produce an undesirable thermally insulating effect that has an adverse impact on the rate of melting. However, feed with fine quartz particle size released gases faster than feed with large quartz particles.

REFERENCES

1. R. Pokorny and P. Hrma, “Model for the conversion of nuclear waste melter feed to glass,” *Journal of Nuclear Materials*, 445, 190-199 (2014).

2. F. C. Johnson, A. S. Choi, D. H. Miller, and D. M. Immel, “Comparison of HLW Glass Melting Rate Between Frit and Glass Forming Chemicals Using X-Ray Computed Tomography,” *SRNL-STI-2014-00562 Revision 0*, Aiken, SC, April 2015, U. S. Department of Energy (2015).

3. P. Hrma, M. J. Schweiger, C. J. Humrickhouse, J. A. Moody, R. M. Tate, T. T. Rainsdon, N. E. Tegrotenhuis, B. M. Arrigoni, J. Marcial, C. P. Rodriguez, and B. H. Tincher, “Effect of Glass-Batch Makeup on the Melting Process,” *Ceramics – Silicaty*, 54 (3) 193-211 (2010).

4. P. Hrma, A. A. Kruger, and R. Pokorny, “Nuclear Waste Vitrification Efficiency: Cold Cap Reactions,” Journal of Non-Crystalline Solids, 358, 3559-3562 (2012).

5. D. R. Dixon, M. J. Schweiger, B. J. Riley, R. Pokorny, and P. Hrma, “Cold-Cap Temperature Profile Comparison Between the Laboratory and Mathematical Model,” WM2015 Conference, Phoenix, AZ, March 15-19 (2015).

6. P. Hrma and S. Han, “Effect of Glass Composition on Activation Energy of Viscosity in Glass-Melting-Temperature Range,” Journal of Non-Crystalline Solids, 358, 1818-1829 (2012).

7. P. Hrma, B. M. Arrigoni, and M. J. Schweiger, “Viscosity of Many-Component Glasses,” Journal of Non-Crystalline Solids, 355, 891-902 (2009).

8. S. H. Henager, P. Hrma, K. J. Swearingen, M. J. Schweiger, J. Marcial, and N. E. TeGrotenhuis, “Conversion of Batch to Molten Glass, I: Volume Expansion,” Journal of Non-Crystalline Solids, 357, 829-835 (2011).

9. P. Hrma, J. Marcial, K. J. Swearingen, S. H. Henager, M. J. Schweiger, and N. E. TeGrotenhuis, “Conversion of Batch to Molten Glass, II: Dissolution of Quartz Particles,” Journal of Non-Crystalline Solids, 357, 820-828 (2011).

10. Z. Hilliard and P. Hrma, “A Method for Determining Bulk Density, Material Density, and Porosity of Melter Feed During Nuclear Waste Vitrification,” to be published in Journal of the American Ceramic Society, (2015).

11. M. J. Schweiger, P. Hrma, C. J. Humrickhouse, J. Marcial, B. J. Riley, and N. E. TeGrotenhuis, “Cluster Formation of Silica Particles in Glass Batches during Melting,” Journal of Non-Crystalline Solids, 356, 1359-1367 (2010).

ACKNOWLEDGMENTS

This work was supported by the U.S. Department of Energy's Waste Treatment & Immobilization Plant Project of the Office under the direction of Albert A. Kruger. The Pacific Northwest National Laboratory is operated for the Department of Energy by Battelle Memorial Institute under contract DE AC05 76RL0 1830.